Trees, Forests and People 15 (2024) 100507

Contents lists available at ScienceDirect

Trees, Forests and People

journal homepage: www.sciencedirect.com/journal/trees-forests-and-people

Land use land cover change and intensity analysis of land transformation in and around a moist semi-deciduous forest in Ghana

Famoussa Dembélé [a,*], Reginald Tang Guuroh [b], Padmore Boateng Ansah [b], Da-Costa Boakye Mensah Asare [c], Sié Sylvestre Da [d], Jeffrey N.A. Aryee [e], Stephen Adu-Bredu [b]

[a] WASCAL Graduate Research Program on Climate Change and Land Use, Kwame Nkrumah University of Science and Technology, Kumasi, Ghana
[b] CSIR-Forestry Research Institute of Ghana, KNUST, P. O. Box UP 63, Kumasi, Ghana
[c] Department of Geomatic Engineering, College of Engineering, Kwame Nkrumah University of Science and Technology, Kumasi, Ghana
[d] WASCAL Competence Center, 06 Box 9507, Ouagadougou 06, Burkina Faso
[e] Department of Meteorology and Climate Science, College of Science, Kwame Nkrumah University of Science and Technology, Kumasi, Ghana

ARTICLE INFO

Keywords:
Bobiri Forest Reserve (BFR)
Remote sensing
Land use/cover
Intensity analysis
Land conversion
Leakage
Ghana

ABSTRACT

Land use land cover change, particularly deforestation has significant implications for global climate and socio-ecological systems as well as resulting ecosystem services from natural systems. In Ghana, the demand for fuel, food, and fibre is projected to be the driver of significant expansion of Croplands/mixed vegetation, resulting in degradation and deforestation of natural ecosystems. This research presents a spatiotemporal analysis of land use/cover change in the Bobiri forest and its surrounding areas in Ghana's moist semi-deciduous forest zone. The study aims to investigate the specific changes in dominant land use land cover (LULC) types in the area using land intensity analyses and to analyse the prevalence of deforestation leakage across the Bobiri Forest Reserve (BFR, a protected area) and its surrounding environs from 1986 and 2022. The study used measured land-cover changes at different levels, including intervals, categories, and transitions. The analysis revealed significant changes in land use intensity across different land classes in the area. The overall rate of land use and land cover change exhibited acceleration, indicating extensive land development throughout the studied periods. Notably, Croplands/mixed vegetation and non-vegetated areas experienced the most gains, while the closed forest class consistently declined. Transitions from forests to Croplands/mixed vegetation were observed, highlighting the conversion of natural vegetation for agricultural purposes. Additionally, the results reveal ongoing leakages in the buffer zone of the BFR as compared to the forest reserve with an annual deforestation rate of (0.64 %) and (0.06 %) respectively from 1986 to 2022, with non-vegetated areas and croplands/mixed vegetation dominating the periphery of protected forest areas. The study recommends implementing policy measures specifically geared towards protecting the buffer zone within a 10 km radius. This is particularly important to the entire buffer zone of the protected area (PA) which is facing deforestation leakage, posing a substantial threat to conservation efforts by exposing the PA to various climatic threats.

1. Introduction

Land cover change is defined in literature as transformations of the biophysical state of the earth's surface, prompted by the interaction of anthropogenic activities and the natural environment impacting the local environment, accumulating into global environmental changes (Frimpong et al., 2023). Land cover change has received major research attention due to its effects on global climate and socio-ecological systems (Asubonteng, 2007; Frimpong et al., 2023; Turner et al., 1995). Land cover change effects on global climate occur through changes in the carbon cycle considering that the terrestrial ecosystem is a major source and sink of carbon. Land transformation also alters the land's ecosystem services, resulting in the vulnerability or otherwise of places and people to climate and economic events (Lambin et al., 2003). There are two types of land cover changes recognized in the literature: total conversions and cover modifications. Total conversion occurs when one land cover type is totally replaced by another, and cover modifications happen when the attributes of a specific land cover type are altered. An

* Corresponding author.
E-mail address: dembele.f@edu.wascal.org (F. Dembélé).

https://doi.org/10.1016/j.tfp.2024.100507

Available online 24 January 2024
2666-7193/© 2024 The Author(s). Published by Elsevier B.V. This is an open access article under the CC BY-NC-ND license (http://creativecommons.org/licenses/by-nc-nd/4.0/).

example of conversion is a shift of a forest cover to agricultural land whereas cover modifications include declines in tree density and species richness. The key driver of land cover change is human management (i.e. land use) but also changes in biophysical factors (Kleemann et al., 2017). Although land cover changes may be monitored at regional or national scale, the key processes of change occur at local hotspots and deforestation appears to be the most prominent change process in tropical countries including Ghana with significant global interest (Addo-Fordjour and Ankomah, 2017).

The process of deforestation commences with a gradual decline of healthy forests through such activities as excessive (and often illegal) logging, slash-and-burn farming, gathering of fuel wood, mining, etc. and climaxes with the occurrence of wildfires, illegal occupation, and/or conversion to other land use/cover types (Asubonteng, 2007). Previous studies conducted in the tropics, specifically in Ghana, have documented the transformation of portions of many protected areas (PA), including the Bobiri Forest Reserve (BFR) to other land use/cover types such as agricultural lands, rangelands, and logging sites. However, habitat loss resulting from deforestation and land-use change serves as a core destructive force in the tropics (Asner et al., 2005; Sanfilippo et al., 2017) and threatens the provisioning of important services from forest ecosystems such as carbon storage, biodiversity conservation among others. Aimed to mitigate habitat loss and associated declines in biodiversity, protected areas are widely considered the cornerstones of modern conservation efforts in the face of rapid anthropogenic change (Adams et al., 2023; Afriyie et al., 2021).

It is worth noting that protected areas in Ghana, have largely, succeeded in halting or at least reducing deforestation activities and land clearing within their designated boundaries (Ajayi et al., 2023). Nevertheless, declaring a protected area "successful" with deforestation rates lower within its boundaries than in its immediate surroundings known as “buffer zone” may be unjustified if deforestation is simply transferred to the protected area’s perimeter. This phenomenon is known as leakage, which happens when land uses that are detrimental to conservation efforts (for example, deforestation) are transferred to areas outside of the PA’s administrative limits (Ewers and Rodrigues, 2008). When this shift occurs in the buffer zone of a PA, it has the potential to alter the composition and structure of vegetation in the PA surrounding environs, potentially restricting the ranges and dispersal capabilities of organisms living within the PA and disrupting other ecological functions (DeFries et al., 2010).

In addition, the effectiveness assessments of PAs can be compromised by leakage patterns, as success is often gauged through a comparison of ecosystem health indicators between the PA and its immediate environs (Ewers and Rodrigues, 2008). The importance of PA buffer zones has been emphasized in Article 8 of the Convention on Biological Diversity (CBD), stating that parties (196 countries) to the convention should “Promote environmentally sound and sustainable development in areas adjacent to protected areas to further the protection of these areas” (CBD, 1992). Buffer zones are also recognized by “Aichi Target 11”, which stresses the importance of integrating site-based conservation actions into the broader environment (CBD, 2010).

Despite acknowledging the impact of PA buffer zones on the success of PA conservation efforts, understanding of the extent of leakages remains limited, with many studies attempting to quantify it globally and examining isolated cases in America, Asia Pacific and Africa which found no widespread evidence of deforestation leakage (Fuller et al., 2019; Lui and Coomes, 2016). However, there is only one study conducted in tropical and subtropical regions, encompassing 55 protected areas including one in Ghana (Assin-Attandanso Game Production Reserve), which observed deforestation leakage (Ford et al., 2020). These studies offer some insight into the land use land cover types that exist around the protected area (land cover maps) and the various transitions that took place within and around the PA.

Therefore, this research examined land use change in the Bobiri Forest Reserve and its surrounding areas (10 km radius around the BFR) within Ghana’s semi-deciduous forest zone from 1986 to 2022. Remote Sensing (RS) and Geographic Information System (GIS) was used to analyse patterns and change in the land cover within the study area. The study aims to investigate the specific changes in dominant land use land cover (LULC) types in the area using land intensity analyses developed by Aldwaik and Pontius (2012), Lambin and Geist (1997) and analyses the prevalence of deforestation leakage within the buffer zone of the PA between1986 and 2022. Understanding the dynamic relationship between land use and forest changes is of critical importance for the sustainable use and management of forest landscapes, and plays a significant role in achieving the Goal 15 of the United Nations’ Sustainable Development Goals, i.e. “protect, restore, and sustainably utilize terrestrial ecosystems, manage forests sustainably, combat desertification, and halt biodiversity loss by 2030”.

2. Material and method

2.1. Description of the study area

The research was conducted in the protected area of Bobiri Forest Reserves (BFR) and its environs (10 km radius around the BFR) located within the moist semi-deciduous forest zone of Ghana. The BFR covers over 54 km^2 (Hall and Swaime, 1981; Hawthorne and Abu-Juam, 1995) (Fig. 1) and is surrounded by communities in the Ejisu Municipal of Ashanti region namely Kubease, Akuokrom, Bomfa, Duampopo, Hwereso, Konongo, New Koforidua, Nobewam, Odumasi, Lowcost, Besease, Donaso, Boankra, and Edwenase. The reserve has been subdivided into management units consisting of butterfly sanctuary, research and strict nature reserve (protected), and production area, which together serve production, tourism, research and conservation functions (Djagbletey et al., 2018). Located between latitudes 6° 33′ 15′’ and 6° 48′ 85′’ N and longitudes 1° 25′ 95′’ and 1° 11′ 35′’ W with a land area of approximately 853.42 km^2, the study area concentrated on the land use/land cover types and their evolutions over time to capture the different land transformations undertaken from 1986 to 2022.

The rainfall pattern in this area is bimodal with a wet semi-equatorial climate. The two rainy seasons occur from March to July and September to late November with a long dry season starting from December to March and a short one in August. The average annual precipitation varies between 1200 and 1750 mm, with yearly temperatures ranging from 20 °C in August to 32 °C in March (Baffour-Ata et al., 2021; Benefoh et al., 2008). The BFR unveils a multifaceted vegetation composition highlighted by dominant species like Mahogany (*Khaya anthotheca*), Sapele (*Entandrophragma cylindricum*), and Wawa (*Triplochiton scleroxylon*), alongside a rich understory including Ofram (*Terminalia superba*) and Wawa trees. The coexistence of these trees suggests a complex and interconnected ecological association, potentially characterized by varying roles in the forest ecosystem such as canopy structure, habitat provision, nutrient cycling, and support of diverse flora and fauna (Djagbletey et al., 2018).

Farming is the leading occupation in the area employing over 68 % of the residents in the fringe communities, whereas the industry sector employs just 8 % in the study area (Benefoh et al., 2008).

2.2. Data acquisition

The study utilized Landsat images, with a spatial resolution of 30 × 30 m, obtained from the United States Geological Survey (USGS) in December 1986, January 2007, and January 2022 (Table 1). The study area experiences significant cloud cover due to prolonged rainy seasons, which presents a challenge in obtaining cloud-free land cover data for a change detection between the three different time steps as mentioned by Marshall et al. (1994), and Oduro Appiah et al. (2021). Consequently, we specifically chose Landsat images captured in the mid-dry season of southern Ghana (i.e., December and January) to ensure minimal or no cloud coverage. In addition, the two months were selected to minimize

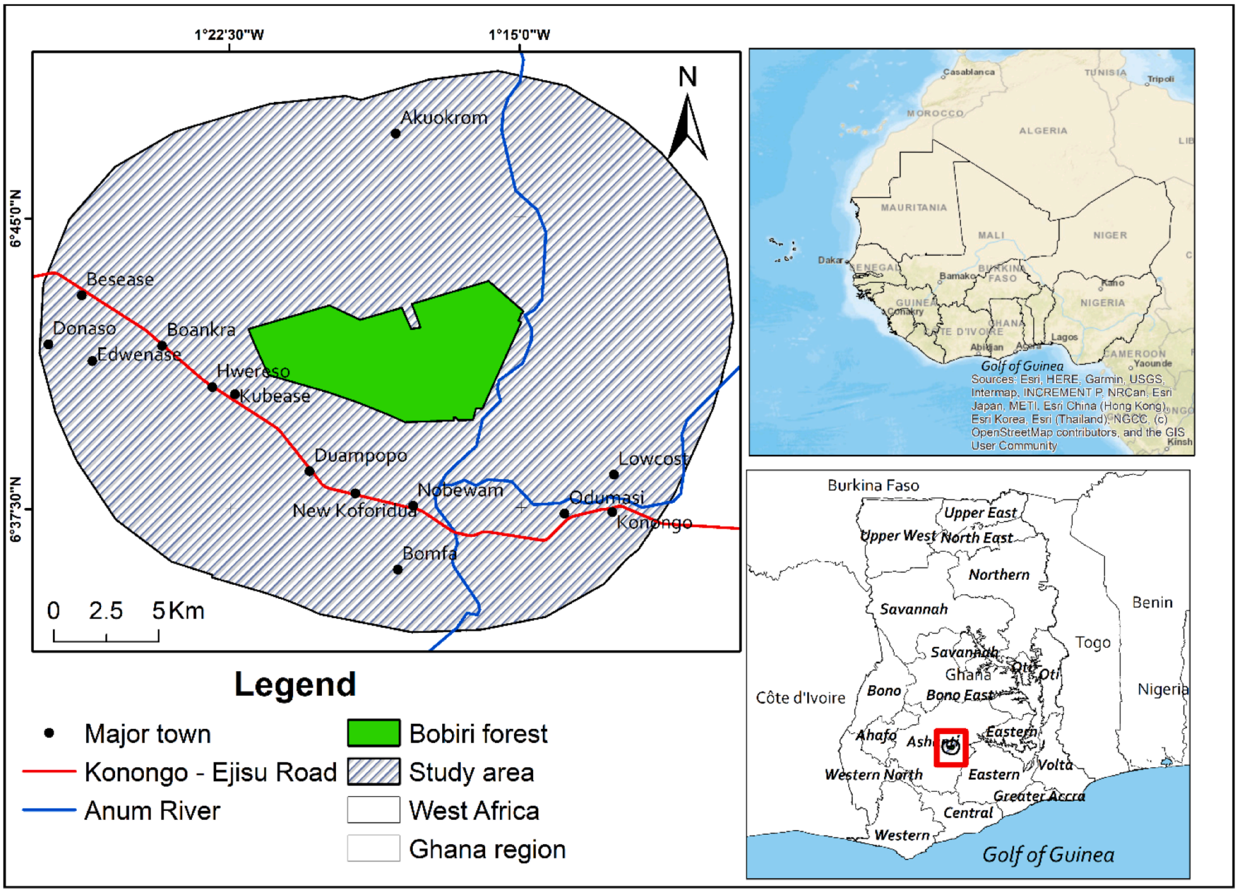

Fig. 1. Map showing the study area (Source of data for map: Environmental Systems Research institute (ESRI) base map, Google Maps and the Resource Management Support Centre of the Forestry Commission of Ghana).

Table 1
Landsat images used and their characteristics.

Image acquisition date	Landsat Sensor	Cell size	Target WRS Path and Row	Projection
22/01/2022	OLI/TIRS 9	30	Path = 194, row = 055	WGS 84 / UTM zone 30N
13/01/2007	ETM+	30	path = 194, row = 055	WGS 84 / UTM zone 30N
29/12/1986	TM 5	30	path = 194, row = 055	WGS 84 / UTM zone 30N

variations resulting from phenological changes in the vegetation. Our objective was to maximize spectral stability to accurately measure changes in land cover around the forest reserve. The change detection analysis of land cover change therefore focused on two intervals: 1986–2007 and 2007–2022. We used images from Landsat Thematic Mapper (TM) 5, Landsat Enhanced Thematic Mapper Plus (ETM+) 7 and Landsat 9 Landsat Operational Land Imager/Thermal Infrared (OLI/TIR) for the years 1986, 2007 and 2022, respectively. For the 2007 image (Landsat 7), we applied a gap filling method using the "Fill no data" tool in QGIS and we used 20 as maximum distance (pixels) to search out for values to interpolate as the study area was affected by the scan-line-corrector error.

Training samples were collected for individual images using different techniques such as normalized difference vegetation index (NDVI), unsupervised classification, as well as band combinations which were applied to the stack band images in QGIS to discriminate some of the land classes from the two images (1986, 2007). The unsupervised classification was performed using the K-mean algorithm in QGIS to create 8 to 10 land classes, which were then reclassified based on their spectral similarity values to form five (5) land classes.

NDVI was calculated using the formula: $NDVI = \frac{(NIR-R)}{(NIR+R)}$, where R is red and NIR is near infrared and has values which range between +1 and -1. Three classification values were set to categorize three land cover types namely, closed forest, open forest and croplands/mixed vegetation. NDVI values between 0.2 and 0.4 were used for croplands/mixed vegetation, between 0.4 and 0.6 were used for open forest and anything above 0.6 was considered as closed forest (EOS, 2019). The range used for croplands/mixed vegetation was that, the images (December and January) used in this study were between the two rainy seasons, during which croplands/mixed vegetation i.e., maize and rice (main crop in the region), and mixed vegetation, such as grasslands and recent fallow lands, exhibit characteristics akin to sparse vegetation. However, NDVI was also used to characterize non-vegetated areas such as build-up, water and bare land. NDVI values between -1 and 0.1 were considered non-vegetated (Hashim et al., 2019). The output of the two methods was compared to select areas of similarity from which 200 polygons were randomly digitized, i.e., 50 polygons each for the 4 land cover classes (Table 2) with each polygon having more than 24 pixels.

However, for the year 2022, field data collection was performed to first acquaint ourselves with the nature of land use within the study area, as well as to choose locations as training datasets for supervised classification. These locations were selected after meeting with the indigenous communities who know the history of their lands. With the help of a handheld GPS, we recorded coordinates of at least 20-squared polygons (at least 50 × 50 m) for each land use type i.e. 80 squared polygons and completed to 200 polygons (30 extra polygons were created for each

Table 2
Definition of the Land-use/cover classes.

Land categories	Definitions	Sources
Closed Forest	This includes all land with woody vegetation consistent with thresholds used to define Forest Land in the national greenhouse gas inventory. It also includes systems with a vegetation structure that currently fall below: - Minimum Mapping Unit (MMU) is 1.0 ha; - Canopy cover (CC) > 65 %; - Potential to reach a minimum height at maturity (in situ) as 5 m.	EPA (2019), Koranteng et al. (2017)
Open forest	This includes perennial crops i.e., oil-palm and cocoa plantations, Orange and fallow areas with similar characteristics that are not considered Cropland and fall below the threshold values used in the Forest Land category such as the other wooded land following the FAO definition in Ghana: CC < 60 %, height ≤ 5 m, MMU > 0.5 ha	EPA (2019)
Croplands and mixed vegetation	This includes annual and biennial croplands such as mono and mixed-cropped farms of cassava, maize, plantain, rice, etc., and recent fallow areas of similar vegetation characteristics.	EPA (2019)
Non-vegetated	This comprises of Cities, towns, villages, and bare areas, rivers, ponds, and lakes.	EPA (2019, Hackman et al. (2017)

land use type) using Google Earth Pro image (see Fig. 2).

2.3. Classification of Landsat images

Supervised classification involves the supervision of the image by an analyst to (smoothen) the pixel categorization process by providing numerical descriptors of the various land cover classes present in a picture to the computer algorithm (Lillesand et al., 2015).

Researchers in LULC change analysis utilize various classification algorithms for satellite image classification. These algorithms encompass both parametric approaches like supervised and unsupervised classification, as well as non-parametric supervised machine learning algorithms. Non-parametric classifiers have become increasingly popular in recent years because of their higher accuracy in image classification, as supported by some studies (e.g. see Lu and Weng, 2007; Qian et al., 2015). While researchers have the freedom to select classifiers based on their judgment, the algorithm's classification accuracy plays a crucial role.

In this study, we use supervised classification; specifically the Random Forest algorithm was employed to classify images, which was done in R 4.2.2 version. The polygons created (50 polygons) for each land use type namely: closed forest, open forest, croplands/mixed vegetation, non-vegetated areas (see Table 2 for a description of the classes) were converted to centroid points i.e., 200 centroid points using the "Feature to Point" tool in ArcGIS.

The Random Forest (RF) classification model was parameterised using the "randomForest" package in R. The process begins by creating a random subset of 1000 sample points of the training dataset (the 200 centroid points) to improve model generalization, from which 70 % was used to train the algorithm and the remaining 30 % for accuracy assessment of the classified images (see Table 3). Key hyper-parameters such as the number of trees, maximum tree depth, and the number of features to consider at any given split were set to 100, 20, and $\sqrt{p}$,

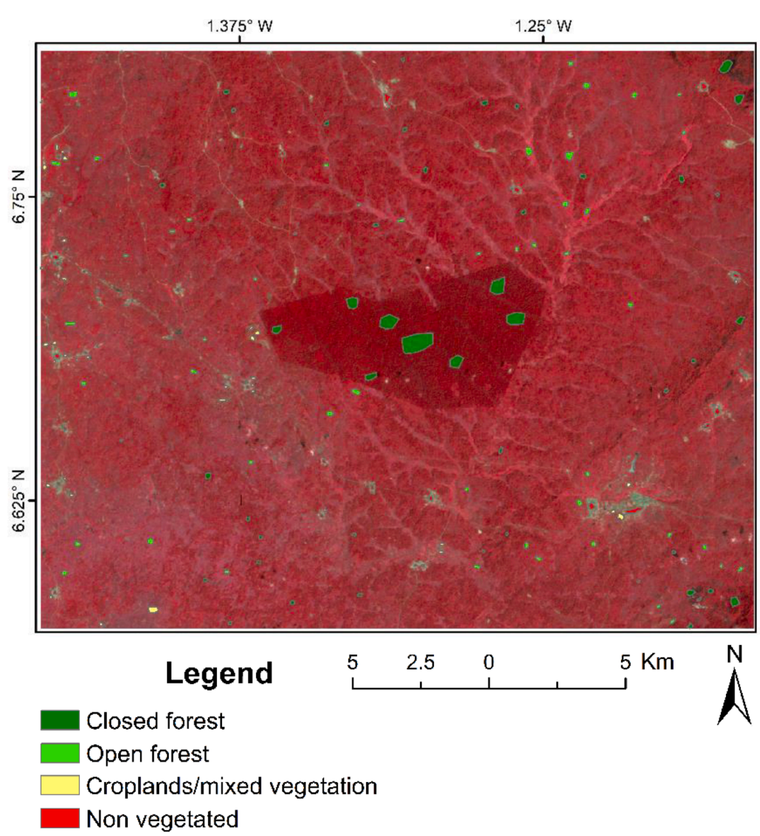

Fig. 2. Training samples distribution on 1986 Landsat 5 image of the study area.

Table 3
The error matrix for the years 1986, 2007 and 2022.

Land use/cover (1986)	Closed forest	Open forest	Croplands/mixed vegetation	Non-vegetated	User Total	User Acc	Producer Acc
Closed forest	161	0	0	0	161	100.00	100.00
Open forest	0	84	2	0	86	97.67	93.33
Croplands/mixed vegetation	0	6	22	1	29	75.86	84.62
Non-vegetated	0	0	2	22	24	91.67	95.65
Producer Total	161	90	26	23	300		
Overall accuracy	***0.96***						
Kappa statistics	***0.94***						
2007							
Closed forest	132	8	1	0	141	93.62	99.25
Open forest	1	95	10	0	106	89.62	88.79
Croplands/mixed vegetation	0	4	20	2	26	76.92	62.50
Non-vegetated	0	0	1	26	27	96.30	92.86
Producer Total	133	107	32	28	300		
Overall accuracy	**0.91**						
Kappa statistics	**0.86**						
2022							
Closed forest	141	4	3	0	148	95.27	97.92
Open forest	3	114	5	0	122	93.44	94.21
Croplands/mixed vegetation	0	3	11	1	15	73.33	55.00
Non-vegetated	0	0	1	14	15	93.33	93.33
Producer Total	144	121	20	15	300		
Overall accuracy	**0.93**						
Kappa statistics	**0.89**						

respectively, where ρ is the number of features/bands. The other parameters were set to the default values in "randomForest" package as described by Breiman (2001); and Griffiths et al. (2014) since they tend to have less impact on predictive accuracy. In this approach, each tree within the Random Forest contributes by voting for the most commonly occurring class based on the input, and the final decision is made through a majority vote across all the trees (Breiman, 2001). This algorithm generates a large number of classification trees (forests) automatically, with each tree based on a random selection of training samples and predictors.

The spectral bands (original) were the predictors. Random Forest avoids the generalisation problems associated with single classification trees by creating many classification trees and thereby enhances classification accuracy (Gislason et al., 2006). Each tree in the forest casts a unit vote for the most popular class. A majority vote of the trees determines the classification result. Random Forest performs internal validation (out-of-bag error rate) on training samples that are not utilised in tree building (Watts and Lawrence, 2008).

The results of the classification were post-processed in ArcGIS 10.3 and QGIS 3.18. The classified images were filtered to eliminate the "salt-and-pepper look" and improve the cartographic appearance. This was accomplished in ArcGIS 10.3 "majority filter" tool using a 3×3 window size. A majority of cells that have the same value and are contiguous were applied for simplifying the map, and eliminating smaller patches of isolated cells. The final land use maps were created using the filtering operation's outputs.

After classification, change statistics were extracted from 1986 to 2007 and 2007 to 2022 maps to produce the two cross tabulation matrices used in change detection analysis.

2.4. Computation of land use land cover changes and intensity analysis

2.4.1. Land transition matrix

Changes in LULC classification were detected through post-classification comparison of maps of the study area from three points in time. Two cross-tabulation matrices were generated for the transitions, one for the 1986 – 2007 interval and the other for the 2007–2022 interval. In the cross-tabulation matrices, the rows display the land-cover types at time t (1986) and columns display the land-cover types at time $t_{+\,1}$ (2007). The inputs in the matrix (P_{ij}) represent the proportion of study area transitioning from land-cover type i at time t to land-cover type j at time $t_{+\,1}$, where $\sum_i \sum_j P_{ij} = 1$.

2.4.2. Intensity analyses

To determine changes in land cover categories, we employed a post-classification change detection method. This technique allowed us to quantify the number of pixels that transitioned from one land category to another. By analysing the intensity of these changes, we calculated the annual percentage change, accounting for both losses and gains in LULC. Additionally, with the assistance of intensity analysis, we assessed changes in land categories at three distinct levels: time interval, categorical, and transition levels, as described by Aldwaik and Pontius (2012). A hypothesised uniform change or intensity is contrasted with an observed change or transition at each level of the analysis. This subsection contains the notations that describe the elements of the equations used to calculate the change or transition at each level of the study.

The equation was built using the following variables; J number of categories; i index for a category at the initial time point for a particular time interval; j index for a category at the final time point for a particular time interval; m index for the losing category in the transition of interest; n index for the gaining category in the transition of interest; T number of time points; t index for the initial time point of interval $[Y_t, Y_{t+1}]$, where t ranges from 1 to $T-1$; Y_t year at time point t; C_{ij} number of pixels that transition from category i at time Y_t to category j at time $[Y_{t+1}]$; (S_t) annual intensity of change for time interval $[Y_t, Y_{t+1}]$; (U) value of uniform annual change/intensity for time-intensity analysis; (G_{tj}) annual intensity of gross gain of category j for time interval $[Y_t, Y_{t+1}]$;

L_{ti} annual intensity of gross loss of category i for time interval $[Y_t, Y_{t+1}]$; R_{tin} annual intensity of transition from category i to category n during time interval $[Y_t, Y_{t+1}]$ where $i \neq n$; (W_{tn}) value of the uniform intensity of transition to category n from all non-n categories at time Y_t during time interval $[Y_t, Y_{t+1}]$; (Q_{tmj}) annual intensity of transition from category m to category j during time interval $[Y_t, Y_{t+1}]$ where $j \neq m$; (V_{tm}) value of uniform intensity of transition from category m to all non-m categories at time Y_t, Y_{t+1} during time interval $[Y_t, Y_{t+1}]$.

Interval level. This level of analysis does not show specific changes of whether there is an increase or decrease in the land categories. However, it gives information on the time intervals during which the overall annual rate of change is relatively slow versus fast. In equation (Eq.) (1), the observed change (S_t) computes the quantity of land cove change (encompassing changes in all land use/land cover classifications) over the research period. Eq. (2) computes the uniform yearly change or intensity (U) for the interval level. The magnitude and rate of change were evaluated at the interval level over time the two time periods (i.e., 1986–2007 and 2007–2022). The rate estimated as the yearly changes spread equally over the full-time span is known as uniform change at interval level. The rate estimated as the change inside each interval spread equally throughout the full geographical range is known as uniform change at the category level. If the observed change (S_t) exceeds the uniform change (U) at the interval level, the change is considered to be rapid. Otherwise, it is slow (Aldwaik and Pontius Jr, 2012).

$$S_t = \frac{\left\{\sum_{j=1}^{J}\left[\left(\sum_{i=1}^{J} C_{tij}\right) - C_{tij}\right]\right\} \Big/ \left[\sum_{j=1}^{J}\left(\sum_{i=1}^{J} C_{tij}\right)\right]}{Y_{t+1} - Y_t} * 100\% \tag{1}$$

$$U = \frac{\sum_{t=1}^{T-1}\left\{\sum_{j=1}^{J}\left[\left(\sum_{i=1}^{J} C_{tij}\right) - C_{tij}\right]\right\} \Big/ \left[\sum_{j=1}^{J}\left(\sum_{i=1}^{J} C_{tij}\right)\right]}{Y_T - Y_1} * 100\% \tag{2}$$

Category level. Category level is computed using Eq. (3) which calculates the gains (G_{tj}) in each of the categories, and Eq. (4) calculates the losses (L_{ti}) in each of the land categories. Eq. (1) calculates a value for uniform intensity for time interval *t* for the category level of the analysis. Therefore, Eq. (1) links the analysis at the interval level to that of the category level. If values of (G_{tj}) were equal for all j, then they would be equal to (S_t). Similarly, if values of (L_{ti}) were equal for all i, then they would be equal to (S_t).

At the category level, if the observed gains and losses are higher than the uniform change (U) see Eq. (2), then the categorical change is active. When the observed change is less than the uniform change, the categorical change is dormant.

$$G_{tj} = \frac{\left[\left(\sum_{i=1}^{J} C_{tij}\right) - C_{tjj}\right] / (Y_{t+1} - Y_t)}{\sum_{i=1}^{J} C_{tij}} * 100\% \tag{3}$$

$$L_{ti} = \frac{\left[\left(\sum_{j=1}^{J} C_{tij}\right) - C_{tii}\right] \Big/ (Y_{t+1} - Y_t)}{\sum_{i=1}^{J} C_{tij}} * 100\% \tag{4}$$

Transition level. The transition level describes the transition (R_{tin}) 'TO' a category from other categories, which is shown and calculated in Eq. (5). The uniform intensity (W_{tn}) of transition to a category n from all the other categories is observed and calculated in Eq. (6). The uniform transition at the transition level is the rate computed as the quantity of land change distributed uniformly among the categories available for the transition (Aldwaik and Pontius, 2012). In case the quantity of land transitions from any of the other categories to n is below a uniform transition intensity (W_{tn}), then n category avoids that particular category. However, when the quantity of land transition from a particular category to n is above the uniform transition intensity, then that category is targeted by n.

$$R_{tin} = \frac{C_{tin}/(Y_{t+1} - Y_t)}{\sum_{j=1}^{J} C_{tij}} * 100\% \tag{5}$$

$$W_{tn} = \frac{\left[\left(\sum_{i=1}^{J} C_{tin}\right) - C_{tnn}\right] / (Y_{t+1} - Y_t)}{\sum_{j=1}^{J}\left[\left(\sum_{i=1}^{J} C_{tij}\right) - C_{tnj}\right]} * 100\% \tag{6}$$

On the contrary of transition 'TO', Eq. (7) below shows how the transition 'FROM' category m to other categories is computed. Its uniform intensity is calculated in Eq. (8).

When the quantity of land transition (Q_{tmj}) from m to another category is under a uniform transition intensity (V_{tm}), then the category m is avoided.

On the other hand, in case the quantity of the transition m is above the uniform transition intensity, the category m is targeted by other land categories.

$$Q_{tmj} = \frac{\left[C_{tmj}/(Y_{t+1} - Y_t)\right]}{\sum_{i=1}^{J} C_{tij}} * 100\% \tag{7}$$

$$V_{tm} = \frac{\left[\left(\sum_{j=1}^{J} C_{tmj}\right) - C_{tmm}\right] \Big/ (Y_{t+1} - Y_t)}{\sum_{i=1}^{J}\left[\left(\sum_{j=1}^{J} Ctij\right) - C_{tim}\right]} * 100\% \tag{8}$$

2.5. Estimation of deforestation leakage

We used the land use/cover maps developed in this study (1986–2022) to calculate the average yearly deforestation rate for BFR and the buffer zones (10 km radius) using ArcMap10.8. From the classification reports generated after the post-classification process ("majority filter"), we quantified deforestation using two different approaches. First, by dividing the area of total closed forest loss between 1986 and 2022 (from the classified image in Fig. 3) by total forested area (closed forest) in year 1986, and expressing as the percentage of year 1986 forested land area that was deforested between 1986 and 2022, known as "deforestation (% forest)" (Eq. (9)). The second approaches quantify deforestation by dividing the area of total closed forest loss between 1986 and 2022 by total terrestrial area (from the classified images in Fig. 3), and expressing as the percentage of terrestrial land area deforested between 1986 and 2022, also known as "deforestation (% land)" (Eq. (10) (Ford et al., 2020; Lui and Coomes, 2016)

$$Deforestation\ (\%\ forest) = \frac{Total\ closed\ forest\ loss\ (1986 - 2022)}{Total\ closed\ forested\ area\ (2022)} \tag{9}$$

$$Deforestation\ (\%\ land) = \frac{Total\ closed\ forest\ loss\ (1986 - 2022)}{Total\ terrestrial\ area\ (2022)} \tag{10}$$

We quantified these two types of deforestation in the study area because both metrics (% forest and % land) provide unique insights into the nature of observed deforestation. The % forest forestation offers insights into absolute rates of closed forest clearing, while the % land deforestation contextualises closed forest loss within the existing forest cover framework, thereby detailing changes in the local availability of forest resources over time. We defined leakage as a higher average yearly deforestation rate in a buffer zone of BFR compared with the PA of BFR (Ewers and Rodrigues, 2008).

3. Results

3.1. Land use/land cover classification

The Random Forest classification technique provided us with good levels of accuracy. The overall accuracies and Kappa statistics for the three maps were 96 %, 91 %, 93 %, and 94 %, 86 %, and 89 % for 1986, 2007 and 2022, respectively. More details on the class performance can be seen in the error matrix (Table 3).

3.2. Land intensity analyses

3.2.1. Interval and category level

The interval level analysis between 1986 and 2007 showed an observed yearly change of 2.06 %, whereas between 2007 and 2022, the area changed by 1.04 % with a uniform change of 1.64 (Fig. 4).

This level of analysis does not show specific changes of whether there is an increase or decrease in the land categories (closed forest, open forest, Croplands/mixed vegetation and non-vegetated). Changes at the category level, on the other hand, were obtained from the interval level of analysis (see Eqs. (3) and (4) and their links with Eq. (1)). The percentage loss in closed forests exceeded that of its gains at the category level in the first interval (see Fig. 5). In both times, Croplands/mixed vegetation, open forest, as well as non-vegetated land, were more likely to increase than decrease.

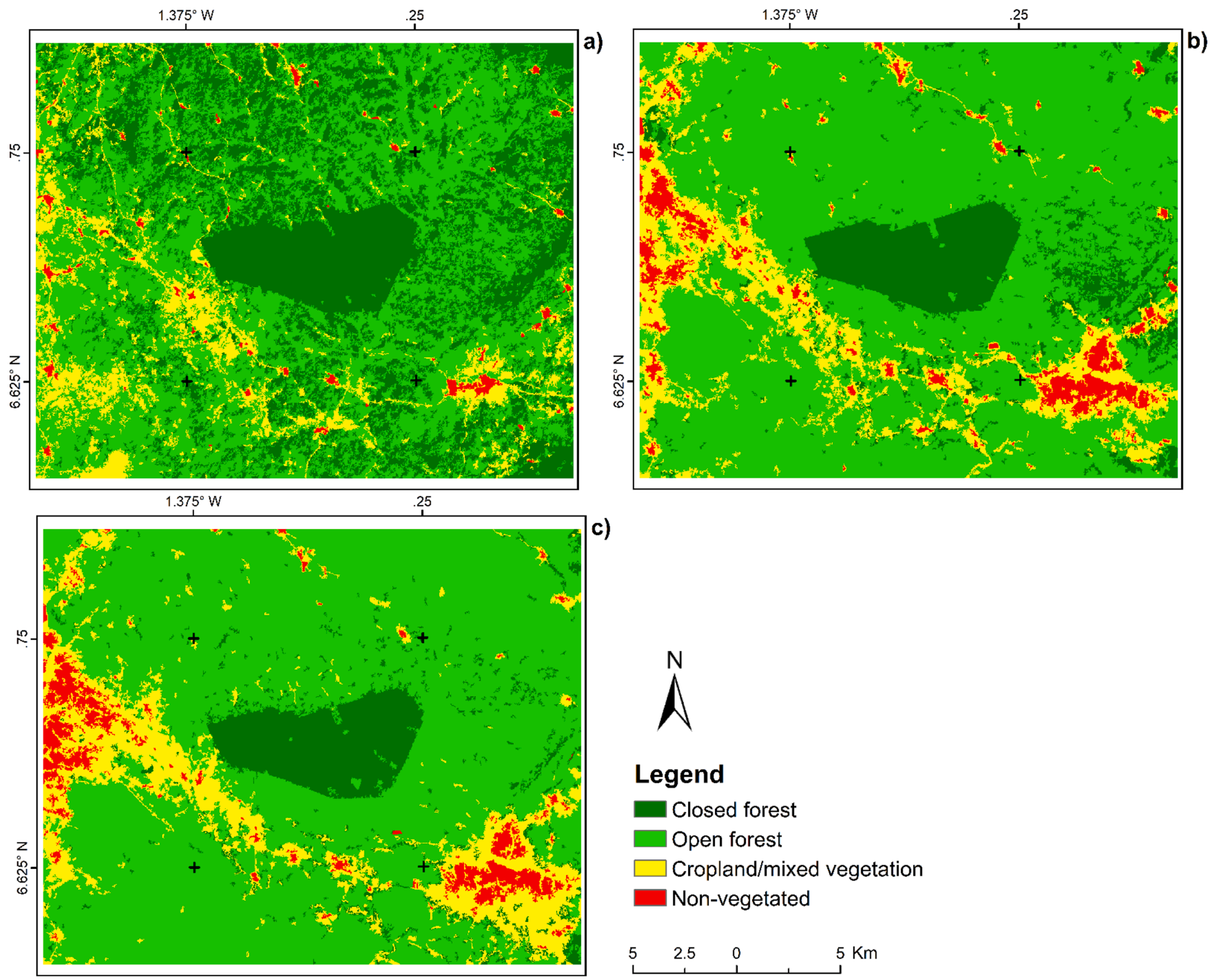

Fig. 3. Land use map of the study area for the years 1986 (a), 2007 (b), and 2022 (c).

In the first period, the net increase in non-vegetated area was more than that in Croplands/mixed vegetation and open forest, while in the second period, the net gain in Croplands/mixed vegetation area was more than that in the non-vegetated and open forest (see Fig. 4).

3.2.2. *Transition level analysis*

This analysis level clarifies the transition between different land use and land cover (LULC) categories by considering whether a specific LULC type was targeted (playing the most significant role in the changes) or avoided (not a primary focus).

An in-depth analysis of landscape transitions within two specific time intervals is provided in Table 5. In the first interval, overall 43 % of the area experienced a change in land use / land cover (LULC), in the second interval (or period) 16 % of the area experienced a LULC change. This change was translated in greatest loss depicted in closed forest and cropland/mixed vegetation with 75 and 60 %, respectively. These losses led to a significant increase in both open forest and non-vegetated areas which expanded from 45,588 to 61,060 ha and 838 to 3243 ha, respectively.

In the same period, it is also important to note that although cropland/mixed vegetation was exposed to losses, it also gained from 9074 to 11,360 ha.

However, when looking at the second period (2007–2022) with an overall change of 16 %, a considerable reduction was observed in the rate of loss in the closed forest and cropland/mixed vegetation as compared to the first interval from 75 to 38 % and from 60 to 34 %, respectively. Furthermore, a fairly stable change can be noticed in open forest and cropland/mixed vegetation from 61,060 to 62,030 ha and from 3243 to 3213 ha, respectively.

It is noteworthy that in the second interval, the rate of loss decreased not only for closed forest but also for Croplands/mixed vegetation, from 75 to 38 % and 60 to 34 %, respectively. This indicates potential changes in land use patterns or ecological processes. Furthermore, Table 5 and Fig. 7 highlight a significant shift in land transition patterns. The magnitude of loss reduces from the first interval to the second interval.

Croplands/mixed vegetation, for example, gained mostly from open forests in both periods. This shows that when compared to all other land use categories, open forest was the most common kind of LULC converted into Croplands/mixed vegetation in both time frames. Various stages of transition from and to other LULC types are seen in Fig. 6.

3.3. *Deforestation rate and potential driving forces*

The deforestation rates calculated throughout the study reveal a total annual deforestation (% forest) rate between 1986 and 2022 of (0.71 %); from which, 0.06 % and 0.64 % occur within the PA and the 10 km

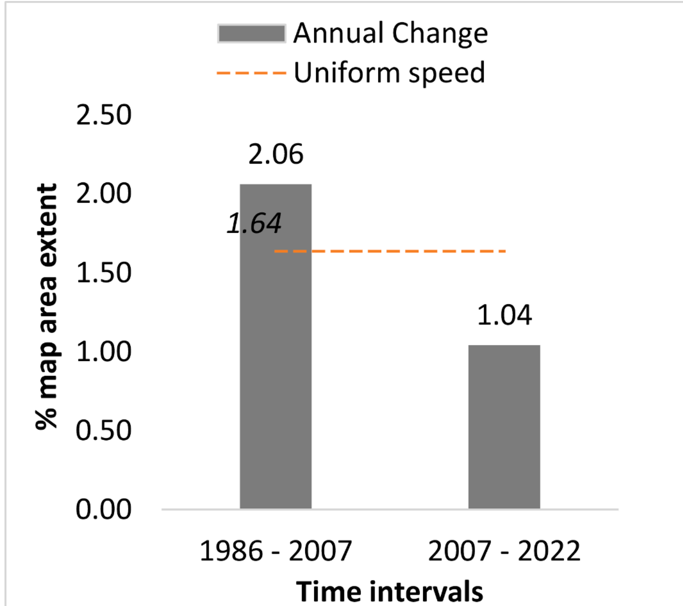

Fig. 4. Interval level analysis.

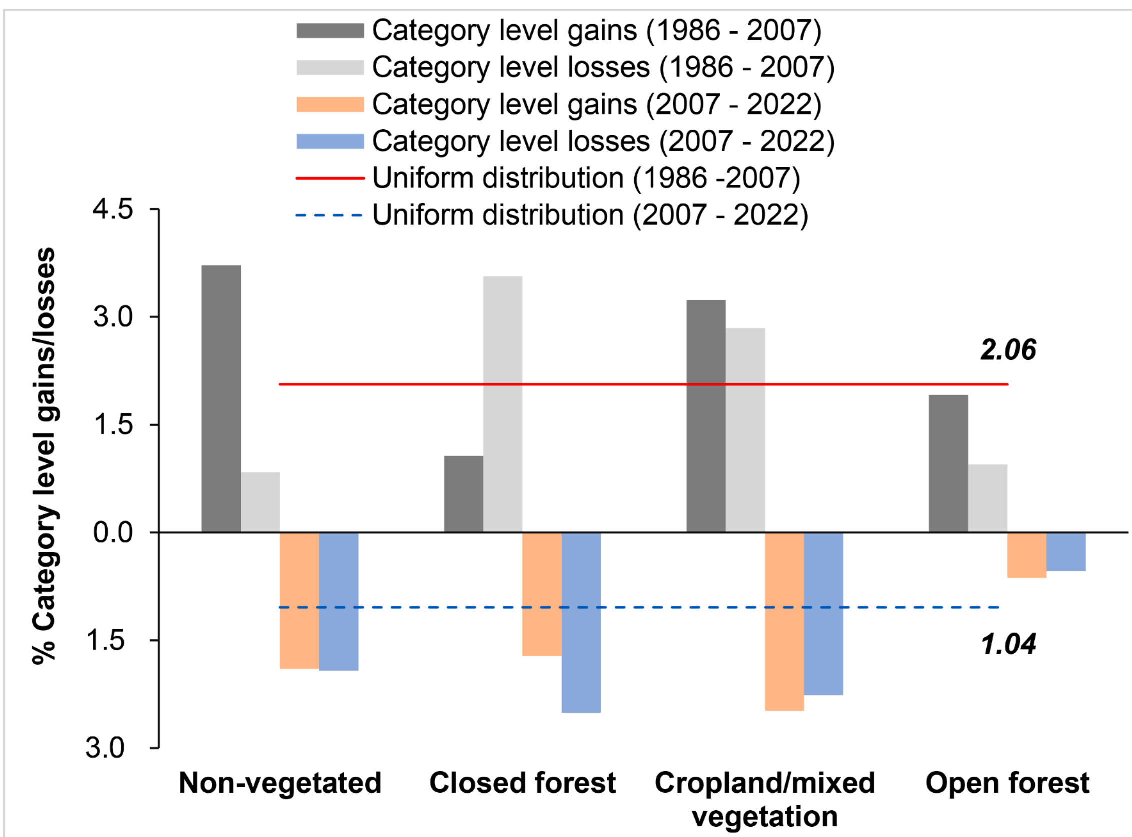

Fig. 5. Category level analysis.

buffer zone of the BFR, respectively. This result suggests a lower deforestation rate in the BFR than in the surrounding buffer zone, which is lower than that found in the annual percentage land deforestation (0.64 %). Therefore, the result provides evidence of leakage in the buffer areas, which experience a rapid decline in closed forest cover than to the wider forest reserve.

4. Discussion

4.1. Land use/cover classification and change detection

Results of the land use/cover classification in this study are consistent with the standard value in the study done by Campbell (2002) with good overall accuracies and kappa statistics, which enables further

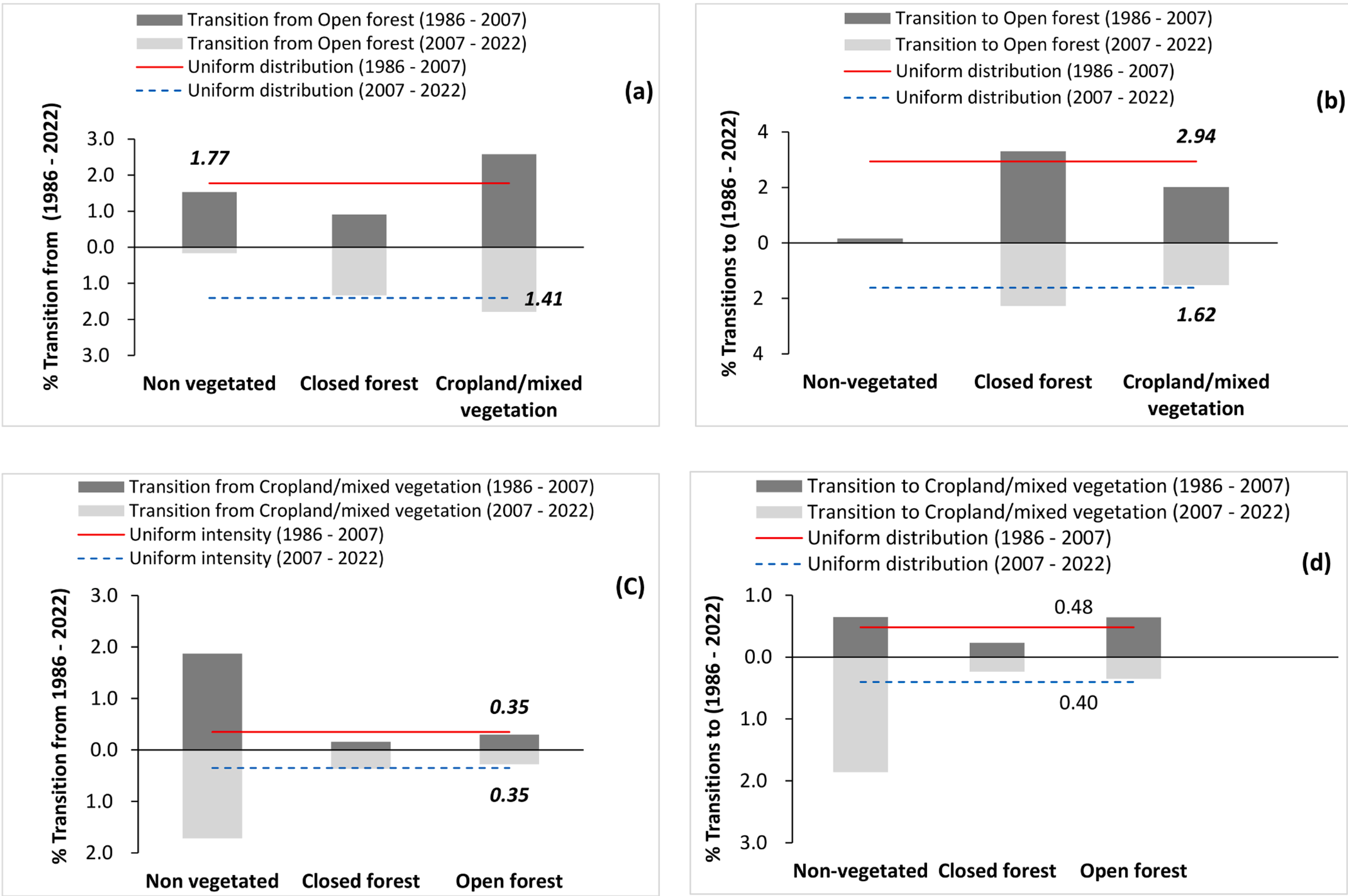

Fig. 6. Analysis of transition intensity (percentage of category) from and to Open forest, Croplands/mixed vegetation and Closed forest and Non-vegetated area across two-time intervals: 1986 – 2007 and 2007 – 2022.

analysis and the formulation of valid conclusions.

Observations of the land use/cover for 1986, 2007, and 2022 reveal a progressive increase in closed forest loss in the buffer zone of BFR over the period. Notably, deforestation-induced forest loss in the study area predominantly occurs outside the boundaries of the designated forest reserves or protected areas (Bobiri forest reserve).

The LULC maps obtained at three different time points displayed four distinct land categories, namely closed forest, open forest, Croplands/mixed vegetation, and non-vegetated areas (primarily comprising buildings and roads). However, a noticeable trend was observed, indicating a decline in the closed forest category, with a corresponding increase in open forest and Croplands/mixed vegetation over the study period 1986 – 2023 (Table 4 and Fig. 3). The analysis of gross change rates revealed significant differences between the two-time intervals (Table 5). Furthermore, the transition tables indicated that the loss of closed forest was accompanied by the expansion of both open forest and Croplands/mixed vegetation. However, the magnitude of change was found to be higher during the first-time interval compared to the second, while transitions from closed forest and non-vegetated areas to Croplands/mixed vegetation decreased (Table 4). The outcomes of this study align with the findings of a similar study by Tekle and Hedlund (2000), who observed a rise in the size of settlements at the expense of forests in the Kalu district of Ethiopia. Similarly, Mark and Kudakwashe (2010) observed a decline in forest cover and an increase in agricultural land in their investigation of the Shurugwi district in the Midlands province of Zimbabwe. The conversion of significant portions of closed canopy forests into open canopy forests within the surrounding of the BFR can be attributed to various underlying factors, such as a decline or inadequacy in forest conservation efforts, rapid socioeconomic developments, and institutional changes (Addo-Fordjour and Ankomah, 2017; Ankomah et al., 2019; Baffour-Ata et al., 2021). In a recent study about the Kyekyewere admitted community within the Tano-Offin Forest Reserve in the Nkawie Forest District, similar trends were observed (Oduro Appiah et al., 2021). On the other hand, the study showed that livelihood activities mainly agricultural expansion, settlements, and harvesting of woody resources are direct drivers of change that flow from the indirect causes, these accounted for the consistent decline in closed forest cover in favour of open forests, and Croplands/mixed vegetation (Oduro Appiah et al., 2021).

4.2. Land use land cover changes and intensity analysis

Previous studies conducted in other countries have compared the intensity analysis method with alternative approaches such as the Markov transition matrix. These studies, including Aldwaik and Pontius Jr. (2012); and Mwangi et al. (2017), have consistently demonstrated that intensity analysis is a highly efficient and effective method for analysing land use changes. Based on these findings, the present study opted to utilize the intensity analysis method to examine the transitional changes among the prominent land categories during the two selected time intervals in the study area. This approach is crucial for gaining insights into the transformations and transitions within the land use land cover (LULC) patterns. The understanding gained from a study of these changes and transitions will aid in formulating policies and implementing interventions that align with the Sustainable Development Goals (SDGs) set forth by the United Nations for achieving sustainable

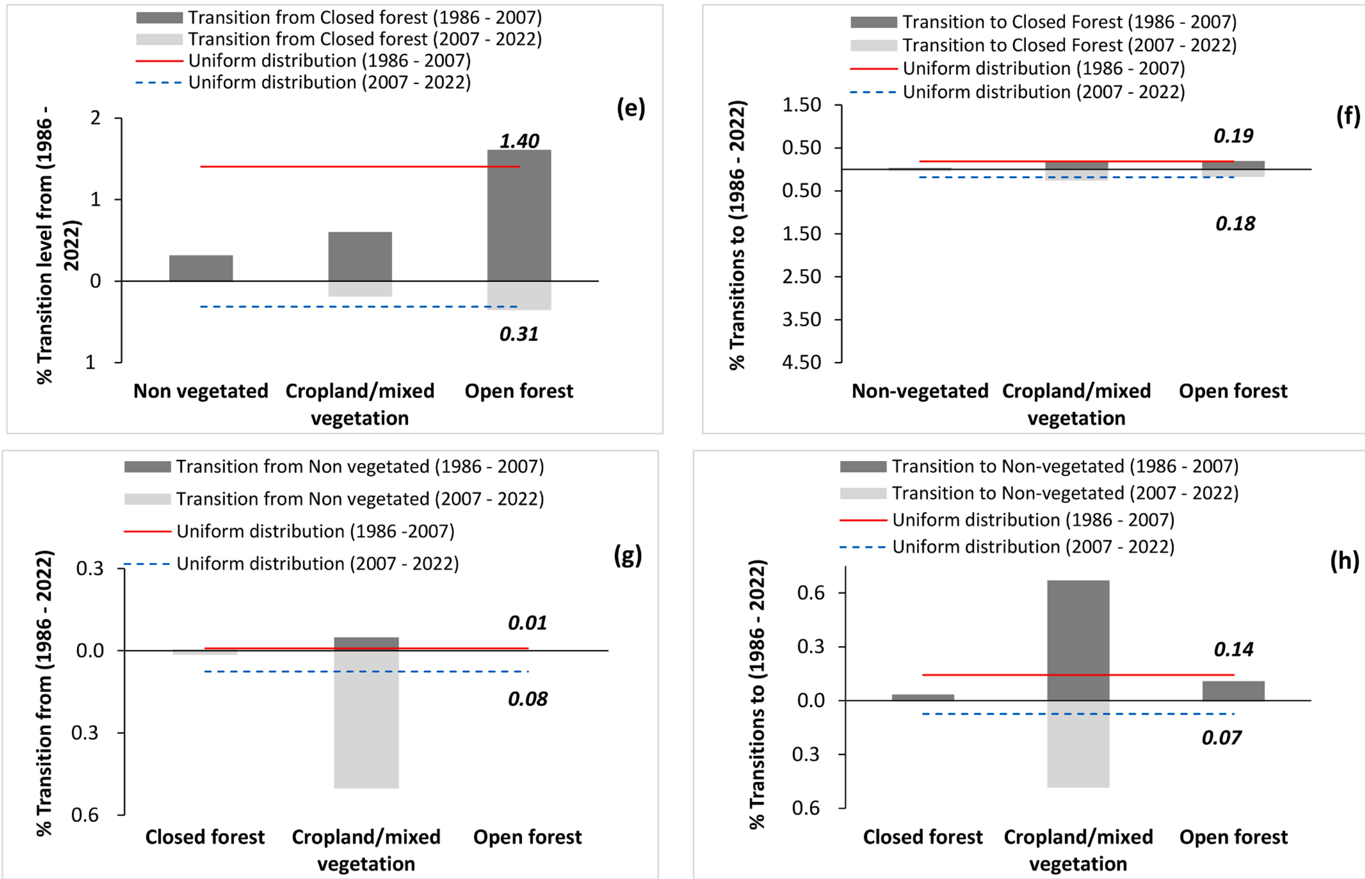

Fig. 6. (*continued*).

development (Christensen and Arsanjani, 2020).

The intensity analysis conducted at the category level revealed noteworthy patterns in LULC. Non-vegetated areas demonstrated active gains throughout all time intervals, while experiencing active losses specifically in the second interval. This trend can be attributed to the upsurge of rural-urban migration, leading to a significant increase in built-up areas within the study region (Nyamekye et al., 2020). The active loss of Non-vegetated areas can primarily be attributed to the expansion of Croplands/mixed vegetation, driven by agricultural activities (Nyamekye et al., 2020).

Croplands/mixed vegetation exhibited active gains in both intervals, which could be due to the rising demand for food resulting from population growth in the study area districts with an increase from 124,176 inhabitants to 244,646 inhabitants between 2000 and 2021 respectively, coupled with consistent reduction in yields (GSS, 2005, 2021). In the case of closed forest, it displayed active losses in both intervals but became an active gainer in the second interval. This later gain in forested land can be attributed to reforestation efforts undertaken by various projects and government initiatives and some agroforestry practices, which transform the cropland into a forest after some years (Table 5).

For example, the National Forest Plantation Development Programme (NFPDP) aimed to accelerate the establishment of new forest plantations by setting a yearly target of 20,000 hectares. These efforts began to demonstrate impacts on vegetation cover in different sites, including the moist semi-deciduous forest zone surrounding the study area (Addo-Danso, 2010; Bosu, 2010; Oduro, 2016).

The transition intensity analysis revealed disparities in the transited class and the corresponding year. It evidenced a reduction in the overall change intensity during the second interval, as depicted in Fig. 4. In the initial time interval, the expansion of Croplands/mixed vegetation influenced both non-vegetated areas and open forests, while the impact on open forests was comparatively less in the subsequent interval, as illustrated in Fig. 6d. These findings indicate that the changes observed were not consistent between the two intervals and were primarily driven by the expansion of Croplands/mixed vegetation, which is supported by previous vegetation studies (Bessah et al., 2019; Shoyama et al., 2018).

Furthermore, the results underscore the ecological importance of the decline in closed forest cover, as it exhibited the most substantial degree of reduction relative to its state in 1986. The intensity of closed forest loss was more prominent during the initial time interval. Additionally, the study revealed heterogeneous effects of open forest expansion on different vegetation types, with closed forests identified as the most susceptible to the ongoing expansion of open forests.

The consistent occurrence of transitions between non-vegetated and Croplands/mixed vegetation during the two analysed time intervals can be attributed to the constraints imposed by urban growth in Ghana, which has limited the expansion of agricultural lands. The transitions, gains, and losses observed predominantly result from the expansion of non-vegetated areas, often at the expense of Croplands/mixed vegetation. It is essential to address the loss of croplands/mixed vegetation from non-vegetated areas (particularly from settlements) as this trend can be attributed to population growth over the years (Bessah et al., 2019; Nyamekye et al., 2020; Shoyama et al., 2018).

The gain in non-vegetated areas are closely linked to significant urban development in the study area, which can be partially attributed to the conversion of Croplands/mixed vegetation in close proximity to towns (Aspinall, 2004; Koranteng et al., 2015; Li et al., 2013; Müller et al., 2010; Nyamekye et al., 2020).

4.3. Drivers of deforestation leakage

Overall, the results of this study suggest a higher prevalence of

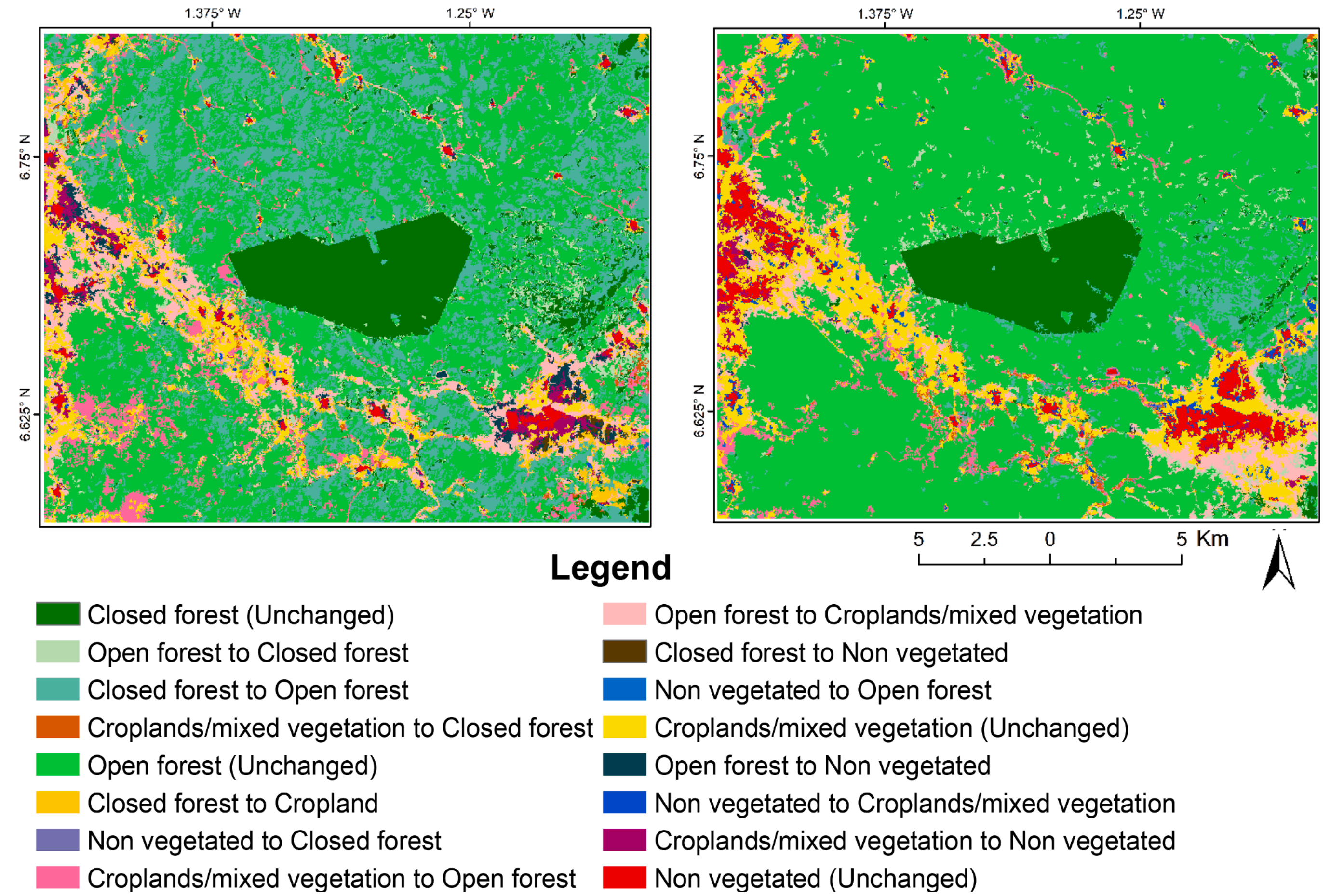

Fig. 7. Change map of the study area between 1986 – 2007 (left image) and 2007 – 2022 (right).

Table 4
Land use change from 1986 to 2007 and 2007 to 2022.

Land use/cover	1986 (ha)	2007 (ha)	2022 (ha)	1st interval net change (ha)	2nd interval net change (ha)	1st interval net change (%)	2nd interval net change (%)	Annual rate of change 1st interval (%)	Annual rate of change 2nd interval (%)
Closed forest	29,805.21	9,641.88	8,100.18	-20,163.33	-1,541.70	-23.64	-1.81	1.13	0.12
Open forest	45,587.61	61,060.14	62,029.62	15,472.53	969.48	18.14	1.14	0.86	0.08
Croplands/ mixed vegetation	9,074.25	11,360.25	11,961.81	2,286.00	601.56	2.68	0.71	0.13	0.05
Non-vegetated	837.81	3,242.61	3,213.27	2,404.80	-29.34	2.79	-0.02	0.13	0.00
Total	85,304.88	85,304.88	85,304.88						

deforestation leakage from the BFR over the study period (1986–2022), with an annual rate of deforestation of (0.64 %) and (0.06 %) for the PA and its 10 km buffer zone, respectively (Table 6). The observed leakage in the study period could be explained by the fact that farmers who have been displaced due to urbanization or peri-urban migration seek alternative Croplands/mixed vegetation, leading to the conversion of forest lands in the buffer areas of the BFR, particularly open forests, in areas located beyond the reach of urbanization. The new Croplands/mixed vegetation are however later replaced with non-vegetated (bareland) when they become unfertile land resulting in the expansion of non-vegetated areas in the buffer zone. The increase in non-vegetated areas is particularly concentrated along the Kumasi-Accra Road network, traversing the study area.

This finding is consistent with the trends documented by (Fisher et al., 2023; Ford et al., 2020), who identified 55 instances of deforestation leakage from PAs in the tropics. In more than 35 cases, agriculture expansion was the dominant driver of forest loss within the buffer zones. Although PAs are typically not created to directly mitigate detrimental land uses beyond their borders, overall conservation success might still depend on activities occurring outside the PA boundaries (DeFries et al., 2010; Laurance et al., 2012). However, in most related studies, we observed a drastic decrease in the protected area forest cover because of deforestation induced by human encroachment into the forest for either built-up (settlement) or farming. From their study in the Ashanti region by analysing patterns of deforestation within some PA to identify main drivers of forest cover loss in the region, Acheampong et al. (2019) reported that agricultural expansion was a major threat to forest cover in the region. Brobbey et al. (2020) also conducted a similar study on three protected areas in Ghana and found agricultural expansion and infrastructure development to be the proximate causes of deforestation. These are driven by population growth, and low productivity of cash crops such as cocoa due to unfertile land. Their study linked the poor

Table 5
Land use land cover transition matrix for two-time intervals: 1986 – 2007 and 2007 – 2022, the numbers represent the percentage of pixels transitioning between categories, with gains and losses calculated by deducting transitions within the same category.

	2007						
	Land use/cover	Closed forest	Open forest	Croplands/mixed vegetation	Non-vegetated	Total	Gross loss (%)
	Closed forest	7480.98	20670.21	1436.49	217.53	29805.21	74.9
	Open forest	1834.83	36532.89	6158.34	1061.55	45587.61	19.86
1986	Croplands/mixed vegetation	319.41	3828.96	3648.69	1277.19	9074.25	59.79
	Non-vegetated	6.66	28.08	116.73	686.34	837.81	18.08
	Total	9641.88	61060.14	11360.25	3242.61	85304.88	
	Gross gain (%)	22.41	40.17	67.88	78.83	**43.32 % Change**	
2022							
	Closed forest	6012.09	3283.83	339.3	6.66	9641.88	37.65
	Open forest	1620.63	56147.13	3213.27	79.11	61060.14	8.05
2007	Croplands/mixed vegetation	446.04	2579.49	7506.9	827.82	11360.25	33.92
	Non-vegetated	21.42	19.17	902.34	2299.68	3242.61	29.08
	Total	8100.18	62029.62	11961.81	3213.27	85304.88	
	Gross gain (%)	25.78	9.48	37.24	28.43	**15.64 % Change**	
2022							
	Closed forest	6553.26	21090.96	1890	270.99	29805.21	78.01
	Open forest	1237.68	36715.23	6401.25	1233.45	45587.61	19.46
1986	Croplands/mixed vegetation	303.12	4195.71	3417.03	1158.39	9074.25	62.34
	Non-vegetated	6.12	27.72	253.53	550.44	837.81	34.30
	Total	8100.18	62029.62	11961.81	3213.27	85304.88	
	Gross gain (%)	19.10	40.81	71.43	82.87	**44.63 % Change**	

Table 6
Summary of deforestation rates from 1986 to 2022 for the designated BFR and its surrounding environs (10 km radius). Deforestation rates are presented as both average annual percentage of land deforested (% land) between 1986–2007 and 2007–2022, and average annual percentage forest deforested (% forest) from 1986 to 2007 and 2007 to 2022.

Regions	1986	2007	2022	% change (1986 - 2022)	% Annual rate of Change
Closed forest (BFR)	5420.18	5415.94	5296.69	**2.26**	**0.06**
Closed forest (Study area)	29737.30	9608.21	8038.80	25.44	0.71
Closed forest (Buffer zone)	24317.12	4192.27	2742.11	**23.18**	**0.64**
Total Land of the BFR	5464.70	5464.70	5464.70		
Total land study area	85304.89	85304.89	85304.89		

fertility and low productivity of cocoa farms as reasons why farmers encroach into the Forest Reserves of Krokosua, Tano Offin and Sui River to increase productivity.

Despite the problem of encroachment of deforestation activities into some forest reserves, the BFR has over the years received relatively good protection. One of the main reasons for its effective conservation is the recognition of its high ecological and tourism value. This has led to constant control by the Forestry Commission (FC) and high research interest in the area evidenced by the long-term presence of researchers. Guards from the Forestry Commission of Ghana regularly monitor the area to detect and prevent illegal logging and other deforestation activities such as mining, and hunting. The long-term presence of researchers (since the year 1946; Djagbletey et al., 2018) has resulted in the protection of a so-called "science safeguarding effect " in which scientists function as de facto park guards (Laurance, 2013)

5. Conclusion

The implementation of intensity analysis in the study area revealed significant changes across the land use classes. The study revealed an overall increased rate of land use and land cover change (LULCC), indicating extensive land development throughout the analysed intervals. Notably, the Croplands/mixed vegetation and non-vegetated classes experienced the largest gains, while the closed forest class consistently experienced losses in both time intervals. The gains in the non-vegetated class primarily originated from Croplands/mixed vegetation, while closed and open forests were comparatively avoided. However, active transitions from closed forest and open forest to Croplands/mixed vegetation were observed in both intervals. Moreover, throughout the three time points, there was active transitioning between the Croplands/mixed vegetation and non-vegetated classes.

Our research highlighted the effectiveness of using contemporary Landsat products to enhance our understanding and assessment of the conservation success of the protected area of Bobiri Forest Reserve in Ghana. Furthermore, the study unveiled a higher prevalence of deforestation leakage within the 10 km buffer zones of the protected area of BFR. Nevertheless, the protected area itself curtails deforestation within its borders, as indicated by an observed annual deforestation rate of 0.06 % throughout the entire study period, compared with a much higher deforestation rate outside the protected area (0.64 %) as what would be expected without protection.

Considering the likelihood that the Protected Area (PA) of the Bobiri Forest Reserve (BFR) will continue to play a crucial role in conservation, we recommend implementing policy measures specifically geared towards protecting the buffer zone within a 10 km radius. This is particularly important to the overall conservation goal of the area, as it would help prevent/reduce deforestation leakage within the buffer zone and reduce substantial threat of exposing the PA itself to various possible encroachment and other climatic threats. Additionally, the global protected area network is formally established in international law through Target 11 of the 2010 Convention on Biological Diversity. However, focusing merely on protecting the boundary of a protected area does not necessarily translate to positive impacts on habitat and biodiversity, if the PA shifts threats to areas where biodiversity is more highly vulnerable. Investigating and managing this potential relocation effect should be a primary focus of research as more protected areas are designated. Our study provides important insights on ensuring more holistic protected area management that would ensure long-term protection and ensure that maximum benefits are derived from such areas. This is important and has applicability for land/ resource managers, conservationists, researchers, and governments.

CRediT authorship contribution statement

Famoussa Dembélé: . **Reginald Tang Guuroh:** Supervision, Visualization, Writing – review & editing. **Padmore Boateng Ansah:** Writing – review & editing. **Da-Costa Boakye Mensah Asare:** Software, Supervision, Writing – review & editing. **Sié Sylvestre Da:** Writing – review & editing. **Jeffrey N.A. Aryee:** . **Stephen Adu-Bredu:** Supervision, Validation, Visualization, Writing – review & editing.

Declaration of competing interest

The authors declare that they have no known competing financial interests or personal relationships that could have appeared to influence the work reported in this paper.

The authors declare the following financial interests/personal relationships which may be considered as potential competing interests:

This work was funded by the German Federal Ministry of Education and Research (BMBF) through the program WASCAL (West African Science Service Center on Climate Change and Adapted Land Use)

Data availability

Data will be made available on request.

References

Acheampong, E.O., Macgregor, C.J., Sloan, S., Sayer, J., 2019. Deforestation is driven by agricultural expansion in Ghana's forest reserves. Sci. Afr. 5 https://doi.org/10.1016/j.sciaf.2019.e00146.

Adams, V.M., Chauvenet, A.L.M., Stoudmann, N., Gurney, G.G., Brockington, D., Kuempel, C.D., 2023. Multiple-use protected areas are critical to equitable and effective conservation. One Earth 6 (9), 1173–1189. https://doi.org/10.1016/j.oneear.2023.08.011.

Addo-Danso, S. D. (2010). Survival and Growth in a Moist-semi Deciduous Forest in Ghana: comparison of monoculture and mixed-species plantations [University of Freiburg]. In Researchgate.Net. https://www.researchgate.net/profile/Shalom-Addo-Danso/publication/265453828_Survival_and_Growth_in_a_Moist-semi_Deciduous_Forest_in_Ghana_comparison_of_monoculture_and_mixed-species_plantations/links/5776b0f208ae1b18a7e1aff7/Survival-and-Growth-in-a-Mois.

Addo-Fordjour, P., Ankomah, F., 2017. Patterns and drivers of forest land cover changes in tropical semi-deciduous forests in Ghana. J. Land. Use Sci. 12 (1), 71–86. https://doi.org/10.1080/1747423X.2016.1241313.

Afriyie, J., Asare, M., Danquah, E., Pavla, H., 2021. Assessing the management effectiveness of three protected areas in Ghana. Conserv. Soc. 19 (1), 19–24. https://doi.org/10.4103/cs.cs_20_28.

Ajayi, E.O., Akin-Idowu, P.E., Aderibigbe, O.R., Ibitoye, D.O., Afolayan, G., Adewale, O. M., Adesegun, E.A., Ubi, B.E., 2023. We are IntechOpen, the world ' s leading publisher of open access books built by scientists, for scientists TOP 1 %. IntechOpen 13. https://doi.org/10.5772/intechopen.109823, 11(tourism).

Aldwaik, S.Z., Pontius, R.G., 2012. Intensity analysis to unify measurements of size and stationarity of land changes by interval, category, and transition. Landsc. Urban. Plan. 106 (2012), 103–114. https://doi.org/10.1016/j.landurbplan.2012.02.010.

Ankomah, F., Kyereh, B., Asante, W., Ansong, M., 2019. Patterns of forest cover change and their association with forest management regimes of forest reserves in the high forest zone of Ghana. J. Land. Use Sci. 14 (3), 242–257. https://doi.org/10.1080/1747423X.2019.1665116.

Asner, G.P., Knapp, D.E., Broadbent, E.N., Oliveira, P.J.C., Keller, M., Silva, J.N., 2005. Ecology: selective logging in the Brazilian Amazon. Science (1979) 310 (5747), 480–482. https://doi.org/10.1126/science.1118051.

Aspinall, R., 2004. Modelling land use change with generalized linear models—a multimodel analysis of change between 1860 and 2000 in Gallatin Valley, Montana. J. Environ. Manage. 72 (1–2), 91–103. https://doi.org/10.1016/j.jenvman.2004.02.009.

Asubonteng, O.K., 2007. Identification of Land Use /Cover Transfer Hotspots in the Ejisu-Juabeng District, Ghana. [Kwame Nkrumah University of Science and Technology]. In Itc. https://webapps.itc.utwente.nl/librarywww/papers_2007/msc/nrm/asubonteng.pdf.

Baffour-Ata, F., Antwi-Agyei, P., Nkiaka, E., 2021. Climate variability, land cover changes and livelihoods of communities on the fringes of bobiri forest reserve, Ghana. Forests 12 (3), 1–24. https://doi.org/10.3390/f12030278.

Benefoh, D. T., Oppong, S., Matthew, E., & Jnr, O. (2008). Spatial mapping of carbon stocks in different land-use /cover types: a case study of Ejisu-Juaben District, Ghana. October.

Bessah, E., Bala, A., Agodzo, S.K., Okhimamhe, A.A., Boakye, E.A., Ibrahim, S.U., 2019. The impact of crop farmers' decisions on future land use, land cover changes in Kintampo North Municipality of Ghana. Int. J. Clim. Chang. Strateg. Manage 11 (1), 72–87. https://doi.org/10.1108/IJCCSM-05-2017-0114.

Bosu, P. P. (2010). Alternative mixed plantation systems and restoration strategies for conservation and sustainable production of native tropical species in Ghana (Issue March). http://www.itto.int/files/itto_project_db_input/2526/Technical/ITTOMIXEDPLANTATIONTechnicalREPORT.pdf.

Breiman, L., 2001. Random forests. Springer Clim. 45, 5–32. https://doi.org/10.1023/a:1010933404324. Leo Breiman (2001). Random Forests. , 45(1), 5–32.

Brobbey, L.K., Agyei, F.K., Osei-Tutu, P., 2020. Drivers of Cocoa encroachment into protected forests: the case of three forest reserves in Ghana. Int. For. Rev. 22 (4), 425–437. https://doi.org/10.1505/146554820831255533.

Campbell, J.B., 2002. Introduction to Remote Sensing (Third Edit). CRC Press, 2002 Taylor \& Francis. https://books.google.com.gh/books?id=1KfQxsN0vp8C.

CBD, 1992. Article 8 in-situ conservation. Text of the Convention on Biological Diversity.

CBD. (2010). X/2.strategic plan for biodiversity 2011-2020. CBD. at: https://www.cbd.int/decision/cop/?id=12268.

Christensen, M., Arsanjani, J.J., 2020. Stimulating implementation of sustainable development goals and conservation action: Predicting future land use/cover change in Virunga national park, Congo. Sustainability (Switzerland) 12 (4). https://doi.org/10.3390/su12041570.

DeFries, R., Karanth, K.K., Pareeth, S., 2010. Interactions between protected areas and their surroundings in human-dominated tropical landscapes. Biol. Conserv. 143 (12), 2870–2880. https://doi.org/10.1016/j.biocon.2010.02.010.

Djagbletey, G.D., Adu-Bredu, S., Duah-Gyamfi, A., Abeney, E.A., Asante, W.A., Akyeampong, E., Addo-Danso, S., Ametsitsi, G.K., Amponsah-Manu, E., Dabo, J., 2018. Floristic composition and carbon stocks of tree species of different conservation status following selective logging in a moist semi-deciduous forest in Ghana. Ghana J. For. 34 (01), 15–34.

EOS, 2019. (2019). NDVI FAQ: all you need to know about index. https://eos.com/blog/ndvi-faq-all-you-need-to-know-about-ndvi/#:~:text=How To Measure Density Of,possible density of green leaves.

EPA. (2019). Ghana ' s fourth national greenhouse gas inventory report. In National Greenhouse Gas Inventory to the United Nations Framework Convention on Climate Change (Issue February). www.epa.gov.gh.

Ewers, R.M., Rodrigues, A.S.L., 2008. Estimates of reserve effectiveness are confounded by leakage. Trends Ecol. Evol. 23 (3), 113–116. https://doi.org/10.1016/j.tree.2007.11.008.

Fisher, J., Allen, S., Woomer, A., Crawford, A., 2023. Protected areas under pressure: an online survey of protected area managers regarding social and environmental conservation target attainment and stakeholder conflicts. World Dev. Sustain. 3, 100084 https://doi.org/10.1016/j.wds.2023.100084.

Ford, S.A., Jepsen, M.R., Kingston, N., Lewis, E., Brooks, T.M., MacSharry, B., Mertz, O., 2020. Deforestation leakage undermines conservation value of tropical and subtropical forest protected areas. Glob. Ecol. Biogeogr. 29 (11), 2014–2024. https://doi.org/10.1111/geb.13172.

Frimpong, F.F., Koranteng, A., Atta-Darkwa, T., Junior, O.F., Niedźwiecki, Z., 2023. Land cover changes utilising landsat satellite imageries for the Kumasi metropolis and its adjoining municipalities in. MDPI. Sensor 23, 2644. https://doi.org/10.3390/s23052644.

Fuller, C., Ondei, S., Brook, B.W., Buettel, J.C., 2019. First, do no harm: a systematic review of deforestation spillovers from protected areas. Glob. Ecol. Conserv. 18 (2019), e00591. https://doi.org/10.1016/j.gecco.2019.e00591.

Gislason, P.O., Benediktsson, J.A., Sveinsson, J.R., 2006. Random Forests for land cover classification. Pattern. Recognit. Lett. 27 (4), 294–300. https://doi.org/10.1016/j.patrec.2005.08.011.

Griffiths, P., Kuemmerle, T., Baumann, M., Radeloff, V.C., Abrudan, I.V., Lieskovsky, J., Munteanu, C., Ostapowicz, K., Hostert, P., 2014. Forest disturbances, forest recovery, and changes in forest types across the Carpathian ecoregion from 1985 to 2010 based on Landsat image composites. Remote Sens. Environ. 151, 72–88. https://doi.org/10.1016/j.rse.2013.04.022.

GSS. (2005). Population data analysis reports. Policy Implications of Population Trends Data, 2(August), 1–495.

GSS. (2021). Ghana 2021 population and housing census.

Hackman, K.O., Gong, P., Wang, J., 2017. New land-cover maps of Ghana for 2015 using landsat 8 and three popular classifiers for biodiversity assessment. Int. J. Remote Sens. 38 (14), 4008–4021. https://doi.org/10.1080/01431161.2017.1312619.

Hall, J.B., Swaime, M., 1981. Distribution and ecology of vascular plants in a tropical rain forest (ed.). In: Junk, W.Dr (Ed.), Forest Veg). The Hague, Netherlands.

Hashim, H., Abd Latif, Z., Adnan, N.A, 2019. Urban vegetation classification with ndvi threshold value method with Very High Resolution (VHR) pleiades imagery. Int. Arch. Photogramm. Remote Sens. Spat. Inf. Sci. XLII-4/W16, 237–240. https://doi.org/10.5194/isprs-archives-XLII-4-W16-237-2019.

Hawthorne, W., Abu-Juam, M., 1995. Forest Protection in Ghana: With Particular Reference to Vegetation and Plant Species. IUCN, ODA/Forest Department Republic of Ghana.

Kleemann, J., Baysal, G., Bulley, H.N.N., Fürst, C., 2017. Assessing driving forces of land use and land cover change by a mixed-method approach in north-eastern Ghana, West Africa. J. Environ. Manage 196, 411–442. https://doi.org/10.1016/j.jenvman.2017.01.053.

Koranteng, A., Adu-poku, I., Zawila-niedzwiecki, T., 2017. Drivers of land use change and carbon mapping in the Savannah area of Ghana Drivers of land use change and

carbon mapping in the savannah area of Ghana. Folia For. Polon. Ser. A 59 (4), 287–311. https://doi.org/10.1515/ffp-2017-0031.
Koranteng, A., Zawiła-Niedźwiecki, T., Kombat, D., 2015. Land use dynamics in rural-urban environs: a study of the Kumasi metropolis and its adjoining districts – Ghana. Teledetekcja Śr. 52, 67–85 ((2015/1)).
Lambin, E.F., Geist, H.J., Lepers, E., 2003. Dynamics of land-use and land-cover change in tropical regions. Annu Rev. Environ. Resour. 28, 205–241. https://doi.org/10.1146/annurev.energy.28.050302.105459.
Lambin, E., Geist, H.J., 1997. Causes of land-use and land-cover change. Washington DC: encyclopedia of earth, environmental information coalition. Natl. Council Sci. Environ. 61 (2), 181–200. http://www.eoearth.org/article/Land-use_and_land-cover_change.
Laurance, W.F., 2013. Does research help to safeguard protected areas? Trends. Ecol. Evol. 28 (5), 261–266. https://doi.org/10.1016/j.tree.2013.01.017.
Laurance, W.F., Carolina Useche, D., Rendeiro, J., Kalka, M., Bradshaw, C.J.A., Sloan, S. P., Laurance, S.G., Campbell, M., Abernethy, K., Alvarez, P., Arroyo-Rodriguez, V., Ashton, P., Benítez-Malvido, J., Blom, A., Bobo, K.S., Cannon, C.H., Cao, M., Carroll, R., Chapman, C., Zamzani, F., 2012. Averting biodiversity collapse in tropical forest protected areas. Nature 489 (7415), 290–294. https://doi.org/10.1038/nature11318.
Li, X., Zhou, W., Ouyang, Z., 2013. Forty years of urban expansion in Beijing: what is the relative importance of physical, socioeconomic, and neighborhood factors? Appl. Geogr. 38, 1–10. https://doi.org/10.1016/j.apgeog.2012.11.004.
In Lillesand, T.M., Kiefer, R.W., Chipman, J.W., 2015. Remote sensing and image interpretation (Eds.). In: Lillesand, T.M., Ralph, R.W., Chipman, J.W. (Eds.), Photogrammetric Engineering & Remote Sensing, 7th Edition. John Wiley & Sons, Inc. https://doi.org/10.14358/pers.81.8.615. (7th ed., Vol. 81, Issue 8).
Lu, D., Weng, Q., 2007. A survey of image classification methods and techniques for improving classification performance. Int. J. Remote Sens. 28 (5), 823–870. https://doi.org/10.1080/01431160600746456.
Lui, G.V., Coomes, D.A., 2016. Tropical nature reserves are losing their buffer zones, but leakage is not to blame. Environ. Res. 147, 580–589. https://doi.org/10.1016/j.envres.2015.11.008.
Mark, M., Kudakwashe, M., 2010. Rate of landuse/landcover changes in Shurugwi District, Zimbabwe: drivers for change. J. Sustain. Dev. Afr. 12 (3), 107–121. https://www.researchgate.net/publication/268370671_Rate_of_land-useland-cover_changes_in_Shurugwi_district_Zimbabwe_drivers_for_change.
Marshall, G.J., Dowdeswell, J.A., Rees, W.G., 1994. The spatial and temporal effect of cloud cover on the acquisition of high quality landsat imagery in the European Arctic sector. Remote Sens. Environ. 50 (2), 149–160. https://doi.org/10.1016/0034-4257(94)90041-8.
Müller, K., Steinmeier, C., Küchler, M., 2010. Urban growth along motorways in Switzerland. Landsc. Urban Plan. 98 (1), 3–12. https://doi.org/10.1016/j.landurbplan.2010.07.004.
Mwangi, H.M., Lariu, P., Julich, S., Patil, S.D., McDonald, M.A., Feger, K.H., 2017. Characterizing the intensity and dynamics of land-use change in the Mara River Basin, East Africa. Forests 9 (1), 1–17. https://doi.org/10.3390/f9010008.
Nyamekye, C., Kwofie, S., Ghansah, B., Agyapong, E., Boamah, L.A., 2020. Assessing urban growth in Ghana using machine learning and intensity analysis: a case study of the New Juaben Municipality. Land. Use Policy 99 (2020), 105057. https://doi.org/10.1016/J.LANDUSEPOL.2020.105057.
Oduro Appiah, J., Agyemang-Duah, W., Sobeng, A.K., Kpienbaareh, D., 2021. Analysing patterns of forest cover change and related land uses in the Tano-Offin forest reserve in Ghana: implications for forest policy and land management. Trees. For. People 5, 100105. https://doi.org/10.1016/j.tfp.2021.100105.
Oduro, K. A. (2016). Ghana ' s high forests : trends, scenarios and pathways for future developments (K. A. Oduro (ed.)). 10.18174/378343.
Qian, Y., Zhou, W., Yan, J., Li, W., Han, L., 2015. Comparing machine learning classifiers for object-based land cover classification using very high resolution imagery. Remote Sens. (Basel) 7 (1), 153–168. https://doi.org/10.3390/rs70100153.
Sanfilippo, M., Akampulira, E., Mohase, A., Okonkwo, H., Ouyoumb, P., Tumber, R., Walmsley, J., Rayment, M., 2017. Reduced impact logging and silvicultural interventions in Ghana: the case of Bobiri forest reserve. Int. For. Rev. 19 (3), 369–380. https://doi.org/10.1505/146554817821865090.
Shoyama, K., Braimoh, A.K., Avtar, R., Saito, O., 2018. Land transition and intensity analysis of cropland expansion in Northern Ghana. Environ. Manage 62 (5), 892–905. https://doi.org/10.1007/s00267-018-1085-7.
Tekle, K., Hedlund, L., 2000. Land cover changes between 1958 and 1986 in Kalu District, Southern Wello, Ethiopia. Mt. Res. Dev. 20 (1), 42–51. https://doi.org/10.1659/0276-4741(2000)020[0042:LCCBAI]2.0.CO;2.
Turner, B.L., Skole, D., Sanderson, S., Fischer, G., Fresco, L., Leemans, R., 1995. Land-Use and Land-Cover Change: Science/Research Plan. International Geosphere-Biosphere Programme. International Geosphere-Biosphere Program "Global Changes, Stockholm.
Watts, J., & Lawrence, R. (2008). Merging random forest classification with an object-oriented approach for analysis of agricultural lands. The International Archives of the Photogrammetry, Remote Sensing and Spatial Information Sciences, 37.